Mechanism of wave-induced liquefaction around suction caissons

Amir Moghaddam[a], Amin Barari[b,*] & Alireza Tabarsa[a]
[a] *Department of Civil Engineering, Golestan University, Gorgan, Iran*
[b] *Department of the Built Environment, Aalborg University, Aalborg, Denmark*

ABSTRACT
Excess pore pressure build-up around offshore foundations may threaten the safety of the foundations. Despite the extensive research effort on mechanism of wave-induced liquefaction around gravity-based foundations and monopile foundations in recent years, there is still a lack of knowledge on mechanism of wave-induced liquefaction around suction caissons. In this paper, CycliqCPSP constitutive soil model implemented in OpenSees is adopted to capture the response of sandy seabed around the suction caisson. Biot's consolidation theory, linear wave theory and the advanced soil model are eventually combined to evaluate the soil response accounting for the hydrodynamic pressure of wave imposed on the seabed surface in the presence of a suction caisson foundation considering the wave-seabed-foundation interaction (WSFI). The results show that occurrence of liquefaction around suction caissons greatly depends on some factors including, initial static stresses, confinement impact of caisson's skirt, drainage path, hydraulic gradient and contact pressure.

RÉSUMÉ
L'accumulation excessive de pression interstitielle autour des fondations offshore peut menacer la sécurité des fondations. Malgré les efforts de recherche approfondis sur le mécanisme de liquéfaction induite par les vagues autour des fondations gravitaires et des fondations monopiles ces dernières années, il y a encore un manque de connaissances sur le mécanisme de liquéfaction induite par les vagues autour des caissons d'aspiration. Dans cet article, le modèle de sol constitutif CycliqCPSP mis en œuvre dans OpenSees est adopté pour capturer la réponse des fonds marins sablonneux autour du caisson d'aspiration. La théorie de consolidation de Biot, la théorie des vagues linéaires et le modèle de sol avancé sont finalement combinés pour évaluer la réponse du sol tenant compte de la pression hydrodynamique des vagues imposée à la surface du fond marin en présence d'une fondation à caisson aspirant compte tenu de l'interaction vague-fond marin-fondation (WSFI). Les résultats montrent que l'occurrence de liquéfaction autour des caissons d'aspiration dépend fortement de certains facteurs, notamment les contraintes statiques initiales, l'impact de confinement de la jupe du caisson, le chemin de drainage, le gradient hydraulique et la pression de contact.

1 INTRODUCTION

Recent studies demonstrated that suction caisson is an economically suitable solution as foundation for offshore wind turbines (Achmus et al. 2013; Barari and Ibsen 2017; Ibsen et al. 2015). Suction caisson is a large, thin-walled hollow cylinder, which is closed at the top and open at the bottom. In comparison with traditional offshore pile, the suction caisson has some substantial advantages including its higher horizontal and lateral loading capacity, environment-friendly setup (slightly less sound pollution and reduced vibration), adaptability to varying offshore soil conditions, and accurate positioning.

In the past decade, due to the wide application of suction caisson and the vital role it plays for the construction of offshore structures, some experimental work has been conducted to investigate the performance of suction caissons under cyclic loading (Barari and Ibsen 2017; Nielsen et al. 2017). Also there are some numerical simulations to evaluate the cyclic response of suction caissons (Barari and Ibsen 2020; Gelagoti et al. 2014; Kourkoulis and Georgiou 2015), though literature is no less immature to investigate the mechanism of wave-induced liquefaction around suction caisson foundation.

Evaluating the stability of offshore foundations is of paramount importance for offshore geotechnical engineers involved in the design of foundations in marine environment. When waves propagate on the surface of sea, they impose hydrodynamic pressure on seabed. These cyclic fluctuations generate excess pore pressure that have been identified as a major factor in analyzing the seabed instability around offshore foundations. If the pore pressure reaches the limit value, the effective stress in seabed vanishes which leads the seabed soil to occurrence of liquefaction stage. To avoid this instability around offshore foundations, it is necessary to study the cyclic behavior of seabed under harsh conditions and in the presence of structure.

Based on the field measurements and experimental observations, two mechanisms for wave-induced liquefaction have been identified (Zen and Yamazaki 1990), which are momentary liquefaction and residual liquefaction. First one is caused by the transient excess pore water pressure when the wave-trough moves on the surface of sea water. Wave-induced pore pressure generates large upward pressure gradients on seabed surface and can transitorily liquefy the soil if the lift induced by upward seepage force surpasses the submerged weight of the seabed soil (Yamamoto et al. 1978). The other is due to the buildup of excess pore water pressure in partially drained or undrained soils caused by the volumetric contraction of soil under cyclic shearing (Seed and Rahman 1978). Residual wave-induced liquefaction is therefore related to the Elasto-plastic behavior of soil. Also assessing the seabed response in the presence of marine structures is more sophisticated because of the existence of initial effective stresses. hence it is of great importance to evaluate the mechanism of wave-seabed-foundation interaction (WSFI) around advanced offshore foundations, including suction caissons due to the complexity in the cyclic behavior of soil in such an environment (Andersen 2015).

In the recent years, most of the wave-seabed-foundation interaction studies have focused on the wave-induced seabed response around gravity-based foundations (Li et al. 2018) and monopile foundations (Tong et al. 2019; Zhu et al. 2018). The study of the wave-seabed-foundation interaction particularly within the scope of suction caissons is quite limited (Zhang et al. 2016).

This paper evaluates the consequence of residual wave-induced liquefaction around suction caisson considering WSFI, using OpenSees, the finite element framework, originally programmed for seismic analysis of structures, soil and SSI (McKenna et al. 2000). To clarify the mechanism of excess pore water pressure accumulation in seabed soil under the action of wave as well as take the Elasto-plastic behavior of seabed soil into account, CycliqCPSP constitutive soil model developed by Zhang and Wang (2012) was used to describe nonlinear characteristic of seabed soil. Biot's consolidation theory, linear wave theory and the advanced soil model were eventually combined to capture the nonlinear response of soil. This finite element numerical model was validated by a well-documented centrifuge test conducted by Sassa and Sekiguchi (1999). To consider the effect of initial state on the process of residual wave-induced liquefaction, a consolidation analysis is completed before performing the dynamic analyses. The results show that occurrence of liquefaction around suction caissons is greatly affected by some factors including, initial static stresses, confinement impact of caisson's skirt, drainage path, hydraulic gradient and contact pressure.

2 THEORETICAL FORMULATION

2.1 Governing equations

The classical Biot's consolidation equations (Biot 1941) are adopted to model the coupling response of soil skeleton and pore water under the action of waves. The saturated soil domain is modeled as a two-phase medium. The equilibrium equation for the soil is defined by

$$\sigma'_{ij} = \sigma_{ij} + \delta_{ij} p \qquad [1]$$

where σ'_{ij} = effective stress, σ_{ij} = total stress, δ_{ij} = Kronecker delta and p = pore water pressure.

According to Biot's consolidation theory, when the accelerations are ignored due to the fluid and soil motion, the governing equation for the porous seabed soil is:

$$\frac{\gamma_w n}{K_f}\frac{\partial P}{\partial t} + \gamma_w \frac{\partial \varepsilon_{ii}}{\partial t} + \nabla^T . [-K_s . (\nabla_P)] = 0 \qquad [2]$$

Where γ_w = unit weight of water, K_f = bulk modulus of the fluid, n = soil porosity, ε_{ii} = the volumetric strain of soil skeleton and K_s = matrix of soil permeability.

Wave-induced excess pore water pressure consists of two components, expressed as follows:

$$P = \breve{P} + \overline{P} \qquad [3]$$

In which P = wave-induced excess pore pressure, $\breve{P}$ = momentary component and $\overline{P}$ = residual component.

According to the linear wave theory, when the waves propagate on the surface of sea, the hydrodynamic pressure imposed on the surface of seabed can be expressed as

$$P_b = \frac{\gamma_w H/2}{\cosh kd}\cos(kx - \omega t) \qquad [4]$$

where P_b = wave pressure, H = wave height, k = wave number, d = water depth and ω = wave frequency.

2.2 Constitutive soil model

In order to give a better prediction of the residual wave-induced liquefaction, it is necessary to consider the stress-strain relationships of the soil particles accompanying the accumulation of pore water pressure within the soil skeleton under the dynamic loading. Hence, the liquefiable sandy seabed is modelled using CycliqCPSP, the Elasto-plastic constitutive soil model for large post-liquefaction shear deformation of sand developed by Wang et al. (2014). The constitutive model works within the bounding surface plasticity framework (Dafalias 1986) to achieve an integrated description of saturated sand of different states from pre-liquefaction to post-liquefaction stages, through applicable formulations for the dilatancy of sand. Parameters of CycliqCPSP constitutive soil model for the simulations are listed in Table 1.

Where G_0 and κ = elastic modulus constants, h = plastic modulus parameter, M, λ_c, e_0 and ξ = critical state parameters, n^p, n^d = state parameter constants, $d_{re,1}$, $d_{re,2}$ = reversible dilatancy parameters, d_{ir}, α, $\gamma_{d,r}$ = irreversible dilatancy parameters.

The constitutive soil model has previously been validated by simulating undrained torsional tests,

undrained and drained triaxial tests, centrifuge model tests and showed successful results, in particular when it used for the purpose of SFI problems in liquefiable soils (Chen et al. 2014, Wang et al. 2016 and Wang et al. 2017). Figure 1 compares the calculated stress path with undrained cyclic torsional test of toyoura with 60% relative density and the result shows the prediction capability of soil model under cyclic loading.

Table 1. Parameters for constitutive soil model

CycliqCPSP	WSFI	Validation
Parameter of elastic shear modulus, G_0	120	80
Parameter of Elastic bulk modulus, κ	0.007	0.006
Plastic modulus parameter, h	0.7	0.6
Critical state stress ratio, M	1.3	1.25
Reversible dilatancy, $d_{re,1}$	0.01	0.01
Reversible dilatancy, $d_{re,2}$	20	10
Reference shear strain, $\gamma_{d,r}$	0.05	0.05
Irreversible dilatancy ratio, α	40	10
Irreversible dilatancy potential, d_{ir}	0.65	0.65
Critical state constant, λ_c	0.021	0.019
Critical state constant, ξ	0.7	0.7
Void ratio at p_c=0, e_0	0.95	1.13
Initial void ratio, e_{in}	0.87	0.85
state parameter constant, n^p	1.1	1.1
state parameter constant, n^d	8	7.8

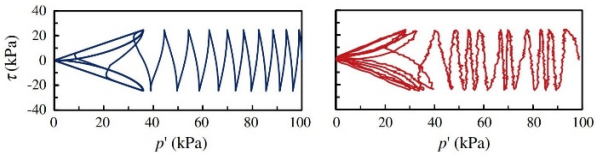

Figure 1. Comparison of the calculated stress path with undrained cyclic torsional test of toyoura sand at Dr = 60% (Wang et al. 2014)

3 NUMERICAL SETUP

3.1 Numerical method

In order to simulate the wave-induced liquefaction around a suction caisson, plane-strain analysis is conducted using the FEM framework, OpenSees.

Based on Biot's theory for porous medium (Biot 1941) and the u-p formulation (Zienkiewicz and Shiomi 1984), the simulation domain can be constructed with the aid of Quadrilateral Four-Node-Quad-UP solid-fluid coupled element which has two displacement degrees of freedom and one pore pressure degree of freedom at each node (Yang et al. 2008). CycliqCPSP Elasto-plastic constitutive model is used to model the liquefiable sandy seabed.

The suction caisson, consisting of lid and skirt, acts as an integrated unit within the seabed soil. Due to the fact that the suction caisson is generally made of steel, it is treated as impervious material by setting its permeability very low (1e-20 m/s). Constitutive model of Elastic-isotropic material is adopted for foundation's domain. Table 2 provides the parameters for the finite-element numerical simulations.

Table 2. Parameters for numerical simulation

Parameters	WSFI	Validation
Wave characteristics		
Wave period, T (s)	7	4.5
Wave height, H (m)	4	1.6
Wavelength, L (m)	47.5	10
Water depth, d (m)	15	4.5
Seabed properties		
Density of soil, ρ_s (kg/m^3)	2000	1860
Permeability of soil, k_s (m/s)	1.7e-5	1e-5
Density of pore water, ρ_w (kg/m^3)	1e3	1e3
Bulk modulus of water, B_f (Pa)	2.2e9	2.2e9
Caisson properties		
Density of steel, ρ_c (kg/m^3)	7850	-
Permeability of caisson, k_c (m/s)	1e-20	-
Elastic modulus, E (Pa)	2e11	-
Poison's ratio, υ	0.3	-
Total length, L_c (m)	7.5	-
Outer diameter, D_c (m)	15	-
Skirt thickness, t_s (m)	0.25	-

Figure 2 shows the FEM mesh used in computation of plain-strain model, in which 6720 elements and 6973 nodes are employed. All of dimensions are illustrated in the scheme. The green lines describe the soil and the red lines describe the suction caisson domain. The configuration is discretized into quad structured mesh with an element size of 0.5 * 0.5 m, while for the caisson and the soil within and beneath the caisson, finer mesh with element size of 0.25 * 0.5 m is used, which helps to achieve more accurate and precise results in these regions.

For the gravitational analysis, the soil model is assigned elastic properties. The soil permeability is set artificially very large (1e0 m/s) to facilitate consolidation while the self-weight of soil and foundation is considered in this step to stablish the initial stress states in the soil.

At the next step, the soil material is set to plastic stage and the soil permeability is updated to its desired value.

For the dynamic analysis, the wave pressure calculated by Equation 4 is imposed on the seabed surface at each time step using the sine time series and plain pattern command, while Newmark method is used as time integrator scheme and numerical simulations showed that a time step of *dt* = 0.01 s is required to appropriately impose the wave pressure on seabed surface. In order to solve the system of equations, ProfileSPD approach along with the Krylov Newton solution algorithm is adopted while rayleigh damping with coefficient of 0.5 is implemented into the model.

Mesh discretization, time steps and model solver were optimized through sensitivity studies. With these considerations, each analysis took about 80 to 120 hours to be completely done using systems with 3.20 and 3.50 GHz processors

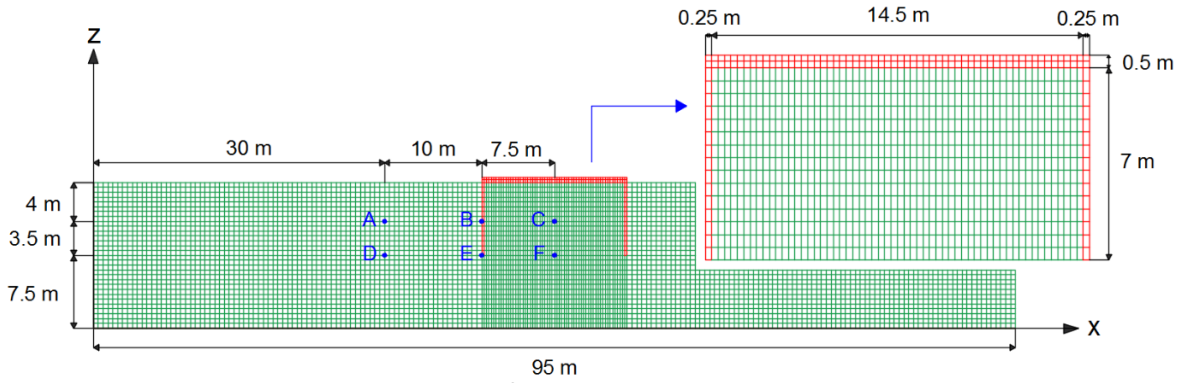

Figure 2. Mesh configuration used in FEM computation

3.2 Boundary conditions

The appropriate boundary conditions are essential for the examination of the wave-induced liquefaction around offshore foundations. The WSFI scheme is shown in Figure 3. The following boundary conditions are applied for the numerical calculation:

1) At the seabed surface the vertical effective stress and shear stress are assumed to be zero. The pore water pressure is equal to dynamic pressure imposed on the seabed surface as in Equation 4.

$$\sigma'_{xx} = \tau_{xz} = 0,\ P = P_b \ \text{at}\ z = h \qquad [5]$$

where τ = shear stress.

2) Periodic boundary is adopted for the lateral sides. Both lateral boundaries are considered to be impermeable (zero-flux), with no displacement in horizontal direction.

$$\frac{\partial P}{\partial x} = 0\ ,\ u_x = 0\ \text{at}\ x = 0\ \text{and}\ x = 2L \qquad [6]$$

In which u_x is horizontal displacement.

3) Since the bottom of seabed is treated as rigid and impermeable, displacements in all directions are fixed and no vertical flow occurs at this bottom boundary.

$$\frac{\partial P}{\partial z} = 0\ ,\ u_x = u_z = 0\ \text{at}\ z = 0 \qquad [7]$$

In which u_z is horizontal displacement.

4) Due to the fact that the suction caisson is generally of steel, it is considered to act as an impermeable boundary in computation. The displacements of caisson in all directions are set to be free to consider the effect of initial stresses which were generated during the consolidation analysis.

$$\frac{\partial P}{\partial n} = 0 \qquad [8]$$

where n is the normal direction to the surface of the caisson's segments.

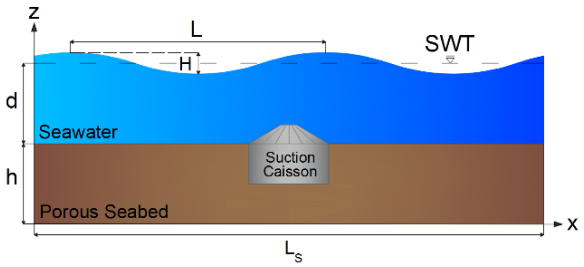

Figure 3. A sketch of the numerical model for the wave-seabed-foundation interaction

4 VALIDATION

OpenSees showed great capability of simulating soil-foundation interaction (SFI) problems in offshore environment (Barari et al. 2017; Ibsen et al. 2014). CycliqCPSP constitutive soil model not only showed the capability of simulating cyclic problems (Section 2), but also is capable to capture the soil response in wave-induced liquefaction problems. Wang and Zhang (2016) showed the feasibility of OpenSees for wave-seabed interaction problems in Poro-elastic seabed. Later, Wang and Zhang (2018) verified adequecies of CyclicCPSP constitutive soil model against wave-seabed-pipeline interaction in Poro-elasto-plastic seabed.

To verify present numerical model, the centrifuge facilities data from Sassa and Sekiguchi (1999) are employed to get a better insight to the capability of FE numerical model in simulating the process of pore pressure accumulation until the liquefaction stage. Figure 4 shows the experimental setup.

Test P5-1 is chosen for the sake of calibration. Model parameters for FE computation are listed in Table 1 and 2. The predictions were carried out in prototype scale. Figure

5 illustrates the numerical predictions excess pore water pressure development over the interval wave passes through the seabed along with experimental data. It could be observed that there is a reasonable agreement between the numerical model and Experimental observation in Sassa and Sekiguchi (1999).

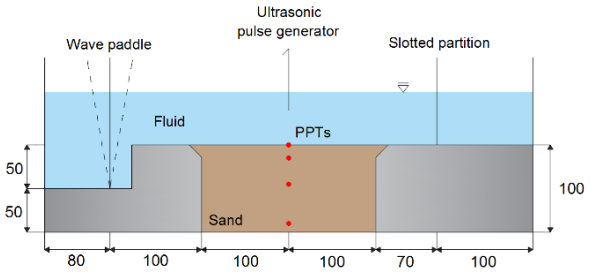

Figure 4. Wave tank used by Sassa and sekiguchi (1999) for centrifuge test (dimensions in mm)

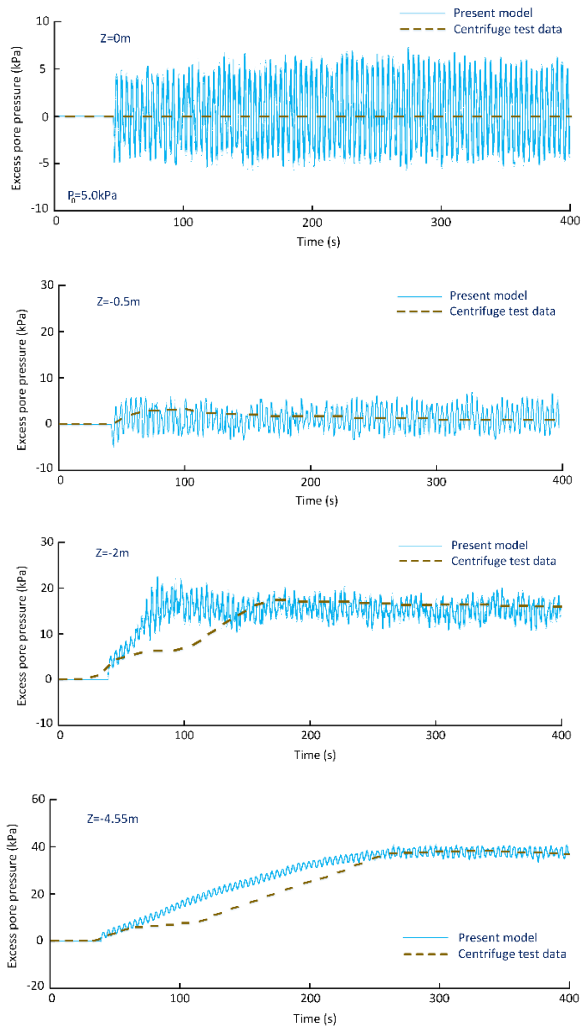

Figure 5. Comparisons of the results between simulated results and experimental data conducted by Sassa and Sekiguchi (1999)

5 RESULTS

5.1 Pore pressure development around suction caisson

In marine environment, the seabed has completed the consolidation stage under seawater hydrostatic pressure and self-gravity. After the installation of suction caisson within the seabed, the soil in the vicinity of foundation, especially under the tip of caisson skirt will be deformed and compressed by the weight of suction caisson. The compression leads to development of excess pore pressure (EPP) in the seabed and by passing the time, excess pore pressure dissipates and suction caisson subsides downward. In the present study, in order to evaluate the mechanism of WSFI problem in Poro-elasto-plastic seabed, the consolidation analysis is completely determined.

The development of excess pore pressure under the foundation during and after dynamic loading depends on factors including: 1) loading intensity; 2) soil properties; 3) foundation contact pressure; 4) foundation's overburden pressure and 5) drainage path (Karimi and Dashti 2016).

The pore water pressure accumulation considering the WSFI is investigated as shown in Figure 6 for three representative moments (i.e., t/T= 5, 15 and 30). It can be observed that the soil around the tip of skirt is a core region in which the pore pressure is much greater than regions at the same depth. It could most likely be attributed to the concentration of large static and cyclic SFI induced shear stresses and shear strains under the tip of suction caisson's skirt.

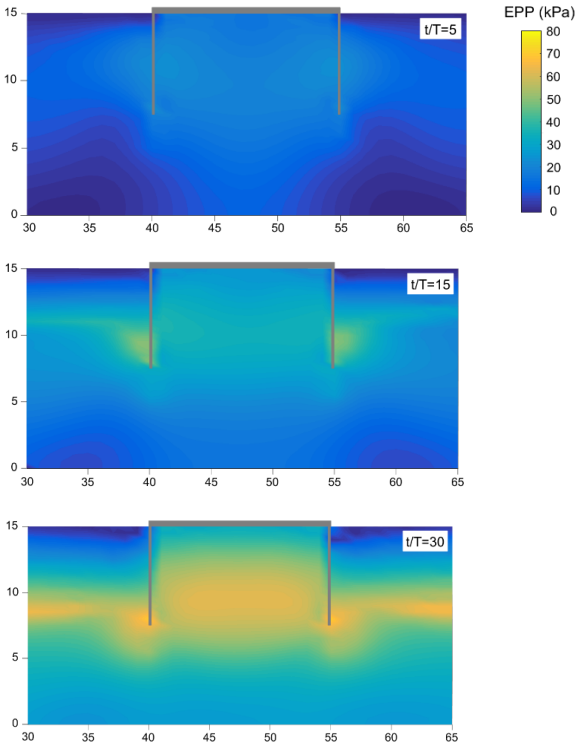

Figure 6. Distribution of the excess pore pressure around the suction caisson (dimensions in m)

There is basically no direct wave loading on the soil within the suction caisson, however the pore pressure build-up is evident during the process of cyclic loading in this region. One reason is that the wave-induced vibration of foundation makes the soil particles within the caisson to re-arrange which leads to slight compression of soil and gradual development of pore pressure.

The other reason is ascribed to the hydraulic gradient. As mentioned above, under the tip of skirt is a core zone for the development of pore pressure. Accordingly the higher pressure in this region makes the pore water to migrate towards regions having lower pressure. When the pore water flows to the soil far away the caisson, it can easily dissipate due to the short drainage path. In contrary, for the higher magnitude excess pore water pressures generated within/underneath the skirts, due to longer drainage path and lateral confinement impact of caisson's skirt and lid, it takes longer to dissipate.

5.2 Residual wave-induced liquefaction around suction caisson

The accumulative compression of the seabed soil under the action of waves may lead to the development of excess pore pressure. When the excess pore pressure reaches the level of the initial effective vertical stress, the seabed loses its shear strength, thus failing to support suction caisson.

The criterion for identifying the residual wave-induced liquefaction in plain-strain condition (Jeng 2013) is adopted as:

$$r_u = \frac{\Delta u}{\sigma'_{v0}} \qquad [9]$$

Where r_u is the excess pore pressure ratio, Δu is the excess pore pressure and σ'_{v0} is the initial effective vertical stress.

In this study, $r_u > 0.95$ is recognized as liquefaction criterion.

In order to gain insight into the process of residual wave-induced liquefaction in the vicinity of suction caisson, 2 rows of points each including 3 points are selected as demonstrated in Figure 3. The first row is located 4 m below the mudline and the second row is 7.5 m below the mudline, where the caisson's skirt ends. Development of r_u for these 6 representative points is depicted in Figures 7 (a) and 7 (b) for 30 cycles of wave loading.

Points A and D (x=30m) are located 10 meters away from the caisson which can represent the free-field response once a comparison with free-field is of interest. Points B and E are exactly located next to the skirt to scrutinize the WSFI problem rigorously. Points C and F are located in the soil within the suction caisson to evaluate the complicated response of soil in this region.

As it can be seen in Figure 7 (a), all points in the depth 4 m below the mudline approximately reached the liquefaction state. It is indicated that r_u of point A suddenly increases after 15 cycles of wave loading and eventually liquefies after 18 cycles. The sudden increase of r_u after 15 cycles can be attributed to the gradual decrease of void ratio in soil from the beginning of cyclic loading.

In contrary to point A, there is no sudden increase in the development rate of r_u for point B which is related to the presence of foundation. The soil in the vicinity of caisson's skirt has experienced a higher level of contact pressure due to the stresses imposed by the overburden load of foundation during the gravitational analysis. So the development of r_u for point B exhibits ever-increasing trend in comparison with point A.

According to Figure 7 (a) and the reasons mentioned in section 5.1, although the maximum amount of pore pressure in the soil within the caisson is higher than far-field in an equal depth, but development of r_u is less in this region. As stated before, liquefaction occurs when the excess pore pressure reaches the level of the initial effective vertical stress. For point C in the soil within the caisson, although, the maximum amount of pore pressure is greater than other points at the same depth, the initial effective vertical stress at this point is higher compared to the other points at the same depth due to the overburden load of caisson's lid and associated contact pressure. Hence, as illustrated in Figure 7 (a), after 30 cycles of wave loading, point C could hardly reach the triggering state of liquefaction.

Results in Figure 7 (a) reveals that the seabed in depth 4 m below the seabed surface reaches residual liquefaction state more quickly when it is closer to the outer surface of caisson's skirt due to the WSFI.

Process of the development of r_u for points D, E and F at depth 7.5 m below the mudline in Figure 7 (b) shows that no liquefaction occurs in this depth after 30 cycles of wave loading. As same as point A, trend of point D is with a slight sudden increase at 22th cycle of wave loading. Although points E and F both have a uniform trend, but after 4 cycles, development rate of point E becomes slightly greater than point F.

A comparison between Figure 7 (a) and 7 (b) reveals that more than 30 cycles of wave loading is required to liquefy the soil at depth 7.5 m below the mudline.

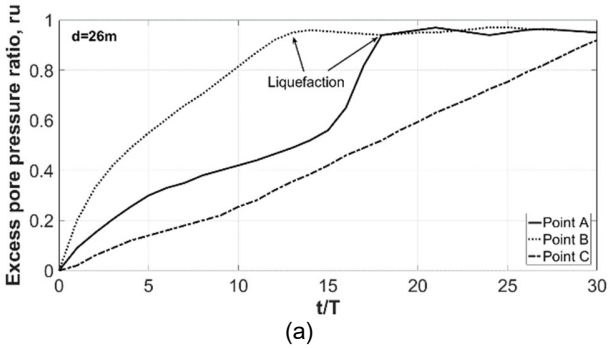

(a)

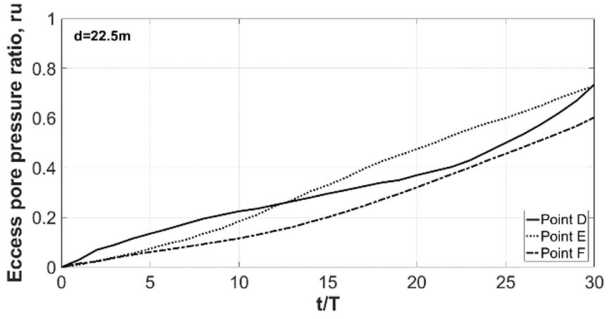

(b)

Figure 7. Pore pressure development at various depths below the mudline: (a) z=11 m (b) z=7.5m

5.3 Effects of wave characteristics on the residual wave-induced liquefaction

The main issues influencing a WSFI problem are: 1) seabed parameters, 2) geometry and material specifications of offshore foundation, 3) wave characteristics and 4) interaction considerations.

Wave period T and wave height H, as two major wave characteristics affecting the development of pore pressure and the wave-induced liquefaction around offshore foundations are considered respectively in this parametric study. The other parameters for numerical simulations are still the same as listed in Table 1.

The excess pore pressure ratio at point B for three different wave periods (T= 5, 7 and 9 s) are demonstrated in Figure 8. Results show that the number of wave loading cycles required for the liquefaction of seabed at point B for wave periods of 5, 7 and 9 s is 16, 15 and 14 respectively. It can be indicated that increasing the wave period has a slight direct effect on the liquefaction potential due to the minor increment in the rate of excess pore pressure ratio.

As it can be seen in figure 9, similar to the the wave period, the wave height has either an obvious impact on the liquefaction potential. Results in figure 9 show that when the wave height increased from 3.5 m to 4.5 m, the number of cycles required for the liquefaction decreased from 18 to 12. Generally speaking, a higher wave height, leads to a higher liquefaction potential.

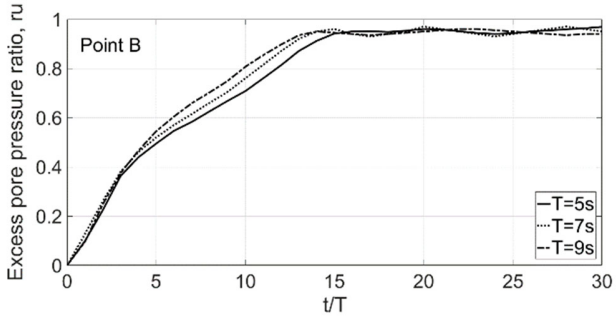

Figure 8. Pore pressure development at point B for the cases with various wave periods, T

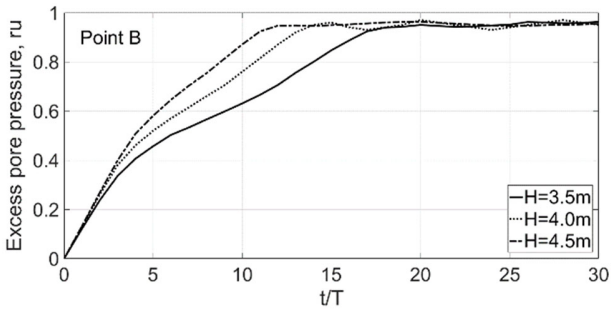

Figure 9. Pore pressure development at point B for the cases with various wave heights, H

6 CONCLUSIONS

In this study, the mechanism of wave-induced liquefaction around suction caisson considering wave-seabed-foundation interaction is evaluated. Biot's consolidation theory, linear wave theory and the elasto-plastic constitutive soil model are eventually combined to capture the soil response in OpenSees finite element software code. The present model is validated by a well-documented centrifuge experimental model. Special attention is paid to the development of pore pressure around the suction caisson and the trend of excess pore pressure ratio in this region. On the basis of the numerical results, the following conclusions can be drawn:

(1) In the case of WSFI problems, it is necessary to conduct the gravitational analysis before performing the cyclic loading, in order to complete the consolidation step and generating the initial static stresses around the offshore foundation.
(2) Around the tip of the caisson's skirt is a core region for the concentration of shear stresses, hence the development of pore pressure in this area is greater in comparison with regions at the same depth.
(3) Although the maximum amount of pore pressure in the soil within the caisson's skirt is higher than far-field in an equal depth, but development of r_u is less in this region. For the soil within the caisson, on one hand, the maximum amount of pore pressure is greater than other points at the same depth. On the other hand, the initial effective vertical stress at is higher compared to the other points at the same depth due to the overburden load of caisson's lid and its contact pressure on the soil within the caisson. Hence, the liquefaction potential of the soil in the region within the caisson's skirt is less than the points in the far-field at the same depth.
(4) The parametric studies demonstrate that an increment in the wave period or the wave height, decreases the number of wave loading cycles required for the liquefaction of the seabed around the offshore foundations. In other words, increases the potential of the wave-induced liquefaction.

REFERENCES

Achmus, M., Akdag, C.T., and Thieken, K. 2013. Load-bearing behavior of suction bucket foundations in sand, *Applied Ocean Research*, 43: 157-165.

Andersen, K.H. 2015. *Cyclic soil parameters for offshore foundation design.* In Frontiers in offshore geotechnics III. CRC Press, Leiden, Netherland. 5-82.

Barari, A. and Ibsen, L.B. 2017. Insight into the lateral response of offshore shallow foundations, *Ocean Engineering*, 144: 203-210.

Barari, A. and Ibsen, L.B. 2020. Investigating the response of tripod suction bucket foundations to multidirectional lateral cyclic loading, *4th International Symposium on Frontiers in Offshore Geotechnics,* University of Texas, Austin, United States.

Barari, A., Bagheri, M., Rouainia, M., and Ibsen, L.B. 2017. Deformation Mechanisms of Offshore Monopile Foundations Accounting for Cyclic Mobility Effects, *Soil Dynamics and Earthquake Engineering*, 97: 439-453.

Biot, M.A. 1941. General Theory of Three-Dimensional Consolidation, *Journal of Applied Physics*, 12(2): 155-164.

Dafalias, Y.F. 1986. Bounding Surface Plasticity; Mathematical Foundation and Hypoplasticity, *Journal of Engineering Mechanics*, 112(9): 966-987.

Foglia, A. and Ibsen, L.B. 2016. Monopod Bucket Foundations Under Cyclic Lateral Loading, *International Journal of Offshore and Polar Engineering*, 26: 109-115.

Gelagoti, F., Kourkoulis, R., Lekkakis, P.C., and Kaynia, A. 2014. Suction caisson foundations for offshore wind turbines subjected to wave and earthquake loading: effect of soil-foundation interface, *Géotechnique*, 64: 171-185.

Ibsen, L., Asgari, A., Bagheri, M., and Barari, A. 2014. Response of monopiles in sand subjected to one-way and transient cyclic lateral loading, *Advances in Soil Dynamics and Foundation Engineering,* Geotechnical Special Publications, ASCE, 312-322.

Ibsen, L.B., Barari, A., and Larsen, K.A. 2015. Effect of embedment on the plastic behavior of bucket foundations, *Journal of Waterway, Port, Coastal, and Ocean Engineering*, 141(6): 06015005.

Kourkoulis, R. and Georgiou, I. 2015. Seismic response of suction caissons: effect of two-directional loading, *6th International Conference on Earthquake Geotechnical Engineering,* WCEE, Christchurch, New Zealand.

Li, Y., Ong, M.C., and Tang, T. 2018. Numerical analysis of wave-induced poro-elastic seabed response around a hexagonal gravity-based offshore foundation, *Coastal Engineering*, 136: 81-95.

McKenna, F., Fenves, G., Scott, M., and Jeremic, B. 2000. Open system for earthquake engineering simulation (OpenSees), PEER Center, Univ. of California, Berkeley, CA, United States, http://opensees.berkeley.edu.

Nielsen, S.D., Ibsen, L.B., and Nielsen, B.N. 2017. Response of cyclic-loaded bucket foundations in saturated dense sand, *Journal of Geotechnical and Geoenvironmental Engineering*, 143(11): 04017086.

Sassa, S. and Sekiguchi, H. 1999. Wave-induced liquefaction of beds of sand in a centrifuge, *Géotechnique*, 49(5): 621-638.

Seed, H.B. and Rahman, M.S. 1978. Wave-induced pore pressure in relation to ocean floor stability of cohesionless soils, *Marine Geotechnology*, 3(2): 123-150.

Tong, D., Liao, C., and Chen, J. 2019. Wave-Induced seabed response around monopile with nonlinear pile-soil interaction, *The 29th International Ocean and Polar Engineering Conference,* International Society of Offshore and Polar Engineers, Honolulu, Hawaii, USA.

Wang, R., Zhang, J.-M., and Wang, G. 2014. A unified plasticity model for large post-liquefaction shear deformation of sand, *Computers and Geotechnics*, 59: 54–66.

Wang, X. and Zhang, J. 2016. Dynamic behaviors of saturated seabed soils induced by different kinds of waves, *OCEANS-2016,* IEEE, Shanghai, China, 1-6.

Wang, X. and Zhang, J.-M. 2018. Interaction of Pipeline and Elasto-Plastic Sandy Seabed Under Dynamic Loadings, *The 28th International Ocean and Polar Engineering Conference,* International Society of Offshore and Polar Engineers, Sapporo, Japan, 7.

Yamamoto, T., Koning, H.L., Sellmeijer, H., and Hijum, E.V. 1978. On the response of a poro-elastic bed to water waves, *Journal of Fluid Mechanics*, 87(1): 193-206.

Yang, Z., Lu, J., and Elgamal, A.-W. 2008. OpenSees Soil Models and Solid-Fluid Fully Coupled Elements, *OpenSees User's Manual,* UC San Diego.

Zen, K. and Yamazaki, H. 1990. Mechanism of wave-induced liquefaction and densification in seabed, *Soils and foundations*, 30: 90-104.

Zhang, J.-F., Zhang, X.-N., and Yu, C. 2016. Wave-induced seabed liquefaction around composite bucket foundations of offshore wind turbines during the sinking process, *Journal of Renewable and Sustainable Energy*, 8(2): 023307.

Zhang, J.-M. and Wang, G. 2012. Large post-liquefaction deformation of sand, part I: physical mechanism, constitutive description and numerical algorithm, *Acta Geotechnica*, 7(2): 69-113.

Zhu, B., Ren, J., and Ye, G.-L. 2018. Wave-induced liquefaction of the seabed around a single pile considering pile–soil interaction, *Marine Georesources & Geotechnology*, 36(1): 150-162.

Zienkiewicz, O.C. and Shiomi, T. 1984. Dynamic behaviour of saturated porous media; The generalized Biot formulation and its numerical solution, *International Journal for Numerical and Analytical Methods in Geomechanics*, 8(1): 71-96.